

Multi-twist optical Möbius strips

Isaac Freund

Physics Department, Bar-Ilan University, Ramat-Gan ISL52900, Israel

Circularly polarized Gauss-Laguerre GL_0^0 and GL_0^1 laser beams that cross at their waists at a small angle are shown to generate a quasi-paraxial field that contains an axial line of circular polarization, a C line, surrounded by polarization ellipses whose major and minor axes generate multi-twist Möbius strips with twist numbers that increase with distance from the C point. These Möbius strips are interpreted in terms of Berry's phase for parallel transport of the ellipse axes around the C point.

OCIS codes: 260.0260, 260.5430, 260.6042, 140.3460.

We show here how to create quasi-paraxial, elliptically polarized light fields in which the major and minor axes of the polarization ellipses generate Möbius strips with radially increasing numbers of half-twists; to our knowledge, these polarization structures are unique.

The polarization ellipses in elliptically polarized *paraxial* fields lie in parallel planes (here the xy -plane) oriented normal to the propagation direction (z -axis). The generic point polarization singularity in any plane of such a field is a C point, an isolated point of circular polarization embedded in a field of polarization ellipses [1 – 5]. The azimuthal orientation of a circle is undefined (singular), and as a result the polarization ellipses surrounding a C point rotate about the point, generically with winding number (net rotation angle/ 2π) $I_C = \pm 1/2$. As the beam propagates in space the C point traces out a line, a C line [1 – 5].

When the beam opens up and is no longer paraxial, the polarization ellipses are no longer constrained to lie in parallel planes; C lines, however, remain. In any plane pierced by a C line a C point appears, and the projections onto the plane of the surrounding ellipses continue to rotate about the point with winding number, or topological charge, $I_C = \pm 1/2$.

What is the full, three-dimensional (3D) arrangement of the ellipses that surround a C line in a *non-paraxial* field? The (possibly surprising) answer is that the major and minor axes of these ellipses generate Möbius strips [6]. The canonical Möbius strip has a single half-twist, and can be either right-handed (RH) or left-handed (LH). Such strips have recently been shown [6] to occur naturally in random fields. Illustrated in Fig. 1 is an example of a left-handed Möbius strip. In random fields left- and right-handed strips are equally probable.

Möbius strips with a larger, odd number of half-twists are possible, and strips with three half-twists are also found in random fields [6]; in such fields $\sim 2/3$ of all Möbius strips have one half-twist, the remainder three half-twists. Optical Möbius strips with more than three half-twists, although not forbidden topologically, do not occur naturally.

Can such strips be generated? The answer is yes, and we show here how to combine two laser beams to create a quasi-paraxial, elliptically polarized beam containing a C

line surrounded by polarization ellipses whose major and minor axes generate Möbius strips with large numbers of half-twists.

An elliptically polarized *paraxial* laser beam containing an axial C line can be generated by a coaxial, coherent superposition of a circularly polarized RH (LH) Gauss-Laguerre GL_0^0 mode and a circularly polarized LH (RH) GL_0^1 mode. The LH (RH) GL_0^1 mode contains a central optical vortex (phase singularity) at which the amplitude vanishes [7], so at that point the polarization in the combined beam is RH (LH) circular. At other points in the beam RH and LH components combine to produce elliptical polarization.

Within the paraxial approximation, at the waists of the individual beams, and therefore at the waist of the combined beam, there exist only the two transverse field components E_x and E_y . However, if the two beams are made to intersect in the xz -plane at small angles $\pm\theta$ relative to the z -axis, a third field component $E_z \sim E_x \sin\theta$ develops. At its waist, the resulting field, described quantitatively below, has the following unique property:

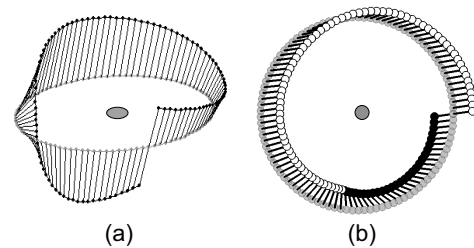


FIG. 1: Computed Möbius strip surrounding a C point in a non-paraxial, elliptically polarized optical field. (a) Three dimensional view of the Möbius strip. Here the major axes of the ellipses on a circle centered on the C point rotate through 180° around the circle circumference to generate a one-half-twist Möbius strip. Throughout, for clarity, only half-axes are shown. (b) The strip in (a) seen from above. In this view ellipse centers are shown by filled gray circles and semi-axes by straight black lines; axis endpoints that lie above (below) the circle of ellipse centers are shown by filled white (black) circles. The ellipse axes can be seen to rotate counterclockwise about the circle circumference, forming a half-turn segment of a left-handed circular screw.

Surrounding the central C point are circular rings of radius r on which the major and minor axes of the polarization ellipses generate multi-twist Möbius strips that contain an odd number of half-twists; these strips have the unique property that *the number of half-twists increases with radial distance r from the C point!*

In Fig. 2 we show an example of such a Möbius strip. In principle, r , and therefore the number of half-twists, increases without limit; in practice, of course, the Gaussian envelope of the beam reduces the intensity to immeasurably small levels far from the beam center.

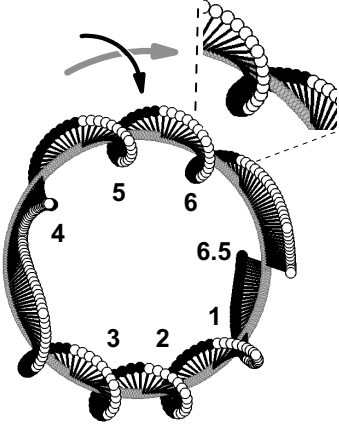


FIG. 2: Computed multi-twist optical Möbius strip generated by the major axes of the polarization ellipses on a circle surrounding a C point. An observer walking (gray arrow) along this circle sees the ellipse axes rotate in the clockwise direction (black arrow), generating a Möbius strip containing 13 half-twists that forms a circular, right-handed screw (helical worm gear) containing 6.5 turns (teeth).

We turn now to a quantitative description of these multi-twist optical Möbius strips. For the sake of definiteness, we take the GL_0^0 mode to be to be RH and the vortex containing GL_0^1 mode to be left handed. We assume that both beams have the same wavelength λ , and the same waist parameter $w_0 \gg \lambda$, and that they intersect maximally at their waists which are centered on the origin. Although there are a number of different experimental approaches to generating such beams, the one most likely to be used involves liquid crystal modulators. These are usually addressed as a Cartesian grid of pixels, and so in what follows we use Cartesian coordinates.

We define a Gaussian envelope function for a GL_0^l beam, $l = 0, 1$, by

$$G_0^l = (w_0/W_0^l) B_0^l \exp\left(-(\rho_0^l)^2 / (W_0^l)^2\right) \times \exp\left(-ik(\rho_0^l)^2 / (2R_0^l)\right) \exp(-ikZ_0^l), \quad (1)$$

where $(\rho_0^l)^2 = (X_0^l)^2 + y^2$, $R_0^l = Z_0^l + 3_0/Z_0^l$, $k = 2\pi/\lambda$, $3_0 = k w_0^2/2$, $W_0^l = w_0 \sqrt{1 + (Z_0^l/3_0)^2}$, $B_0^l = (1 + iZ_0^l/3_0) / \sqrt{1 + (Z_0^l/3_0)^2}$. Writing θ_0^l for the angle that the GL_0^l beam makes with the z -axis,

$$X_0^l = x \cos \theta_0^l + z \sin \theta_0^l, \quad Z_0^l = -x \sin \theta_0^l + z \cos \theta_0^l. \quad (2)$$

The field components of the combined beam $\mathbf{E} = E_x \hat{\mathbf{x}} + E_y \hat{\mathbf{y}} + E_z \hat{\mathbf{z}}$, with $\hat{\mathbf{x}}, \hat{\mathbf{y}}, \hat{\mathbf{z}}$ unit vectors along the corresponding coordinate axes, are

$$E_x = (E_0^0)_x + (E_0^1)_x, \quad E_y = (E_0^0)_y + (E_0^1)_y, \\ E_z = (E_0^0)_x \sin \theta_0^0 + (E_0^1)_x \sin \theta_0^1, \quad (3)$$

where

$$(E_0^0)_x = G_0^0, \quad (E_0^0)_y = iG_0^0, \quad (4a)$$

$$(E_0^1)_x = \sqrt{2}G_0^1 B_0^1 (X_0^1 + i\sigma y) / W_0^1, \quad (4b)$$

$$(E_0^1)_y = -i\sqrt{2}G_0^1 B_0^1 (X_0^1 + i\sigma y) / W_0^1. \quad (4c)$$

In Eqs. (4b) and (4c) $\sigma = +1$ ($\sigma = -1$) for a positive (negative) vortex. For all figures presented here, $w_0 = 100\lambda$, $\theta_0^0 = -\theta_0^1 = 5^\circ$, and $\sigma = +1$.

The major axis α and minor axis β of the ellipses surrounding the C point in Figs. 1 and 2 (and Figs. 3 and 4 below), are obtained from Berry's formulas [5]: $\alpha = \text{Re}(\mathbf{E}^* \sqrt{\mathbf{E} \cdot \mathbf{E}})$, $\beta = \text{Im}(\mathbf{E}^* \sqrt{\mathbf{E} \cdot \mathbf{E}})$.

The exact r dependence of the number of half-twists and handedness of the Möbius strips requires an analyses that is too complicated to describe here. Instead, insight into what happens can be obtained by considering the angle $\alpha_{xy} = \arctan(\alpha_y, \alpha_x)$ shown in Fig. 3, where α_x and α_y are the x, y -components of α . Because α is a line, not a vector, it is plotted modulo π . On the small circle at the center of the figure α_{xy} winds around the central C point, which in such plots appears as a vortex, with winding number $I_C = -1/2$: $I_C = -1/2$ because along a counterclockwise, by convention positive, circuit, α_{xy} decreases by π .

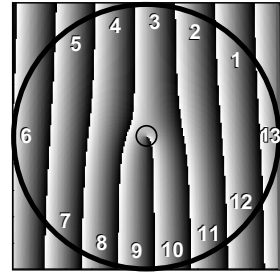


FIG. 3: Rotation angle α_{xy} , plotted 0 to π black to white, of the projection of the major axes α onto the xy -plane.

The corresponding Möbius strip, shown in Fig. 1, can be interpreted in terms of Berry's phase [8]: as one moves along the circle surrounding the C point, α undergoes parallel transport, rotating through π during one complete circuit; this leads to winding number I_C in the xy -projection, and the one-half-twist Möbius strip in 3D.

In addition to the central C point, Fig. 3 contains a number of π -fringes that are analogous to the 2π -fringes in the forked-fringe method for measuring vortices [9, 10]. Each time α passes through a π -fringe it rotates through π , so that the total number of half-twists equals the total number of fringes traversed during a circuit about the C

point. The large circle in Fig. 3 that passes through 13 π -fringes corresponds to the Möbius strip in Fig. 2, which has 13 half-twists. Similar considerations apply to axis β , and in Fig. 4 we show a Möbius strip generated by this axis which has 29 half-twists (14.5 full twists).

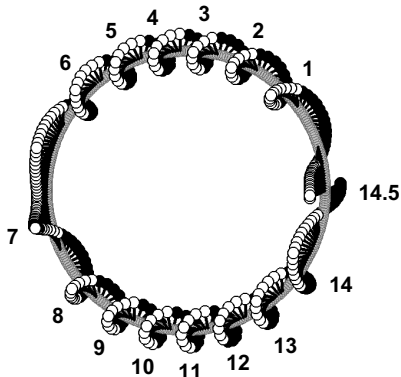


FIG. 4: Möbius strip containing 29 half-twists generated by minor axis β . Here radius $r = 42\lambda$ is twice that of Fig. 2.

The forgoing leads to a simple, heuristic expression for twist number τ , the number of *full* twists, as a function of the radial distance $r \ll w_0$ from the C point. For $\theta_0^0 = -\theta_0^1 = \theta$, far from the C point the fringe spacing along the here horizontal x -axis, is $s = \lambda / (2 \sin \theta)$, so that the number of fringes traversed by a line of length $2r$, the circle diameter, is $2r/s$. On a circle centered on the C point the circumference passes through each fringe twice, and upon adding in the extra π -fringe induced by the C point we obtain

$$\tau_{calc} \simeq \text{int}(4r \sin(\theta) / \lambda) + 1/2. \quad (5)$$

In Fig. 1, $r = 2\lambda$, $\tau_{calc} = 0.5$, in Fig. 2, $r = 20\lambda$, $\tau_{calc} = 6.5$, and in Fig. 4, $r = 42\lambda$, $\tau_{calc} = 14.5$ – in each case in agreement with Eq. (5). We find Eq. (5) to be in general agreement with our computer simulations for $r < w_0/2$; for larger r , s begins to decrease significantly with increasing r due to wavefront curvature and the Gouy phase shift, and Eq. (5) underestimates the twist number.

To be reported on elsewhere are the twist number and handedness of the Möbius strips as a function of r and other system parameters, the n -foil knots generated by the axis endpoints of n -twist Möbius strips, the strips (twisted ribbons) with an even number of half-twists that appear on circles that do not enclose a C point, the multi-twist optical Möbius strips that are generated by other combinations of laser modes, and by other beam configurations, and the z dependence of these structures.

In summary, we have shown how to combine two circularly polarized laser beams, one of which contains a vortex, to create a quasi-paraxial field containing a central C point surrounded by polarization ellipses whose major and minor axes generate multi-twist optical Möbius strips with twist numbers that increase radially from the C point. These Möbius strips are structurally stable, changing unimportantly when, for example, 3% noise is

added to the simulation. Coherent nanoprobe techniques [11–18] capable of determining the field structure on sub-wavelength scales should permit experimental measurements of these highly unusual objects. As for possible applications, we note, inter alia, that the Möbius strips could be embedded in polarization sensitive photoresists to create devices with unique optical properties.

email address: freund@mail.biu.ac.il (I. Freund).

References

- [1] J. F. Nye, *Natural Focusing and Fine Structure of Light* (IOP Publ., Bristol, 1999).
- [2] J. F. Nye, Proc. Roy. Soc. Lond. A **389**, 279–290 (1983).
- [3] M. V. Berry and M. R. Dennis, Proc. Roy. Soc. Lond. A **457**, 141–155 (2001).
- [4] M. R. Dennis, Opt. Commun. **213**, 201–221 (2002).
- [5] M. V. Berry, J. Opt. A **6**, 675–678 (2004).
- [6] I. Freund, “Optical Möbius strips in three-dimensional ellipse fields: I. Lines of circular polarization,” Opt. Commun. in press, doi:10.1016/j.optcom.2009.09.042 (2009).
- [7] M. S. Soskin and M. V. Vasnetsov, “Linear theory of optical vortices,” in *Optical Vortices*, M. Vasnetsov and K. Staliunas Eds., Horizons in World Physics **228**, 1–35 (Nova Science Publs., Commack, New York, 1999).
- [8] An excellent review of Berry’s phase in optics is given in E. J. Galvez, “Applications of geometric phase in optics,” available from Wikipedia (Berry’s phase), or <http://departments.colgate.edu/physics/faculty/galvez.htm>.
- [9] N. B. Baranova, B. Ya Zel’dovich, A. V. Mamaev, N. Pilipetskii, and V. V. Shkukov, JETP Lett. **33**, 195–199 (1981).
- [10] I. V. Basistiy, M. S. Soskin, and M. V. Vasnetsov, Opt. Commun. **119**, 604–612 (1995).
- [11] R. Dandliker, I. Marki, M. Salt, and A. Nesci, J. Optics A **6**, S189–S196 (2004).
- [12] P. Tortora, R. Dandliker, W. Nakagawa, and L. Vaccaro, Opt. Commun. **259**, 876–882 (2006).
- [13] C. Rockstuhl, I. Marki, T. Scharf, M. Salt, H. P. Herzig, and R. Dandliker, Current Nanoscience **2**, 337–350 (2006).
- [14] P. Tortora, E. Descrovi, L. Aeschmann, L. Vaccaro, H. P. Herzig, and R. Dandliker, Ultramicroscopy **107**, 158–165 (2007).
- [15] K. G. Lee, H. W. Kihm, J. E. Kihm, W. J. Choi, H. Kim, C. Ropers, D. J. Park, Y. C. Yoon, S. B. Choi, H. Woo, J. Kim, B. Lee, Q. H. Park, C. Lienau C, and D. S. Kim, Nature Photonics **1**, 53–56 (2007).
- [16] Z. H. Kim and S. R. Leone, Opt. Express **16**, 1733–1741 (2008).
- [17] R. J. Engelen, D. Mori, T. Baba, and L. Kuipers, Phys. Rev. Lett. **102**, 023902 (2009); Erratum: *ibid.* 049904 (2009).
- [18] M. Burrelli, R. J. Engelen, A. Opheij, D. van Oosten, D. Mori, T. Baba, and L. Kuipers, Phys. Rev. Lett. **102**, 033902 (2009).

References with titles

- [1] J. F. Nye, *Natural Focusing and Fine Structure of Light* (IOP Publ., Bristol, 1999).
- [2] J. F. Nye, “Lines of circular polarization in electromagnetic wave fields,” *Proc. Roy. Soc. Lond. A* **389**, 279–290 (1983).
- [3] M. V. Berry and M. R. Dennis, “Polarization singularities in isotropic random vector waves,” *Proc. Roy. Soc. Lond. A* **457**, 141–155 (2001).
- [4] M. R. Dennis, “Polarization singularities in paraxial vector fields: morphology and statistics,” *Opt. Commun.* **213**, 201–221 (2002).
- [5] M. V. Berry, “Index formulae for singular lines of polarization,” *J. Opt. A* **6**, 675–678 (2004).
- [6] I. Freund, “Optical Möbius strips in three-dimensional ellipse fields: I. Lines of circular polarization,” *Opt. Commun.* in press, doi:10.1016/j.optcom.2009.09.042 (2009).
- [7] M. S. Soskin and M. V. Vasnetsov, “Linear theory of optical vortices,” in *Optical Vortices*, M. Vasnetsov and K. Staliunas Eds., Horizons in World Physics **228**, 1–35 (Nova Science Publs., Commack, New York, 1999).
- [8] An excellent review of Berry’s phase in optics is given in E. J. Galvez, “Applications of geometric phase in optics,” available from Wikipedia (Berry’s phase), or <http://departments.colgate.edu/physics/faculty/galvez.htm>.
- [9] N. B. Baranova, B. Ya Zel’dovich, A. V. Mamaev, N. Pilipetskii, and V. V. Shkukov, “Dislocations of the wave-front of a speckle-inhomogeneous field (theory and experiment),” *JETP Lett.* **33**, 195–199 (1981).
- [10] I. V. Basistiy, M. S. Soskin, and M. V. Vasnetsov, “Optical wavefront dislocations and their properties,” *Opt. Commun.* **119**, 604–612 (1995).
- [11] R. Dandliker, I. Marki, M. Salt, and A. Nesci, “Measuring optical phase singularities at subwavelength resolution,” *J. Optics A* **6**, S189–S196 (2004).
- [12] P. Tortora, R. Dandliker, W. Nakagawa, and L. Vaccaro, “Detection of non-paraxial optical fields by optical fiber tip probes,” *Opt. Commun.* **259**, 876–882 (2006).
- [13] C. Rockstuhl, I. Marki, T. Scharf, M. Salt, H. P. Herzig, and R. Dandliker, “High resolution interference microscopy: A tool for probing optical waves in the far-field on a nanometric length scale,” *Current Nanoscience* **2**, 337–350 (2006).
- [14] P. Tortora, E. Descrovi, L. Aeschmann, L. Vaccaro, H. P. Herzig, and R. Dandliker, “Selective coupling of HE11 and TM01 modes into microfabricated fully metal-coated quartz probes,” *Ultramicroscopy* **107**, 158–165 (2007).
- [15] K. G. Lee, H. W. Kihm, J. E. Kihm, W. J. Choi, H. Kim, C. Ropers, D. J. Park, Y. C. Yoon, S. B. Choi, H. Woo, J. Kim, B. Lee, Q. H. Park, C. Lienau C, and D. S. Kim, “Vector field microscopic imaging of light,” *Nature Photonics* **1**, 53–56 (2007).
- [16] Z. H. Kim and S. R. Leone, “Polarization-selective mapping of near-field intensity and phase around gold nanoparticles using apertureless near-field microscopy,” *Opt. Express* **16**, 1733–1741 (2008).
- [17] R. J. Engelen, D. Mori, T. Baba, and L. Kuipers, “Subwavelength Structure of the Evanescent Field of an Optical Bloch Wave,” *Phys. Rev. Lett.* **102**, 023902 (2009); Erratum: *ibid.* 049904 (2009).
- [18] M. Burrelli, R. J. Engelen, A. Opheij, D. van Oosten, D. Mori, T. Baba, and L. Kuipers, “Observation of Polarization Singularities at the Nanoscale,” *Phys. Rev. Lett.* **102**, 033902 (2009).